VOLUME 121, NUMBER 21
JUNE 2, 1999

JOURNAL OF THE AMERICAN CHEMICAL SOCIETY

Effects of Surface Adsorption and Confinement on the Photochemical Selectivity of Previtamin D_3 Adsorbed within Porous Sol−Gel Derived Alumina

Forrest S. Schultz*,† and Marc A. Anderson‡

Contribution from the Department of Chemistry and Water Chemistry Program, University of Wisconsin—Madison, Madison, Wisconsin 53706

Received February 11, 1998

Abstract: It has been demonstrated that porous sol−gel derived (SGD) alumina can function as an effective microorganized medium in which to perform size- or shape-selective organic transformations. For the photolysis of 7-dehydrocholesterol (7D) encapsulated within SGD-alumina, it was found that the adsorption characteristics of 7D and the pore size of the SGD-alumina greatly influenced the photochemical selectivity of the cis−trans isomerization of previtamin D_3 to tachysterol$_3$. An increase in the ratio of previtamin D_3 (P_3) to tachysterol$_3$ (T_3) was obtained on photolysis of 7D adsorbed within SGD-alumina with a pore size of 10−20 Å. This result is attributed to a confinement effect that inhibits the cis−trans isomerization of P_3 to T_3. In addition to the confinement effect on the photochemical selectivity, it was found that the adsorption characteristics of 7D to the surface of SGD-alumina also play a critical role in the photochemical selectivity. The results indicate that confinement in addition to chemisorption via the 3-hydroxyl group of 7D to the surface of activated SGD-alumina is necessary to optimize the photochemical selectivity. The presented results also provide direct experimental evidence to demonstrate that adsorption solely to a metal oxide surface via the 3-hydroxyl group is not sufficient to inhibit the cis−trans isomerization of P_3 to D_3.

Introduction

Many investigators have invested significant efforts to develop systems of microorganized media to increase the selectivity of chemical reactions. With these systems, chemical selectivity has been achieved by confining a reactive chemical species within an organized structure that can limit the conformational flexibility of reactants or transition states leading to different products. Micelles,[1] vesicles,[2] adsorbed mono- and multilayers,[3] molecular crystals,[4] liquid crystals,[5] zeolites,[6] clays,[7] cyclodextrins,[8] organic polymers,[9] nonporous silica and alumina,[10] and semiconductors[11] are a few representative examples of microorganized media. Studies of these systems have produced encouraging results that demonstrate the utility of carrying out

† Department of Chemistry. Current address: Department of Chemistry, University of Wisconsin−Stout, Menomonie, WI 54751.

‡ Water Chemistry Program.

(1) (a) Thomas, J. K.*Chem. Rev*. **1980**, *80,* 283. (b) Turro, N. J.; Cox, G. S. Paczkowsky, M. A. *Top. Curr. Chem.* **1985**, *129*, 57. (c) de Mayo, P.; Sydnes, L. K. *J. Chem. Soc., Chem. Commun*. **1989**, 994.

(2) (a) Takagi, K.; Sawaki, Y.; Crit. Rev. *Biochem. Mol. Biol*. **1993**, *28*, 323−367. (b) Suddaby, B. R.; Brown, P. E.; Russell, J. C.; Whitten, D. G. *J. Am. Chem. Soc*. **1985**, *107*, 5609−5617.

(3) Spooner, S. P.; Whitten, D. G. In *Photochemistry in Organized and Constrained Media*; Ramamurthy, V., Ed.; VCH: New York, 1991; Chapter 15 and references therein.

(4) (a) Scheffer, J. R.; Pokkuluri, P. R. Chapter 5. In *Photochemistry in Organized and Constrained Media*; Ramamurthy, V., Ed.; VCH: New York, 1991. (b) Zimmerman, H. E.; Zuraw, M. J. *J. Am. Chem. Soc*. **1989**, *111*, 2358. (c) Zimmerman, H. E.; Zuraw, M. J. *J. Am. Chem. Soc*. **1989**, *111*, 7974. (d) Ramamurthy, V.; Venkatesan, K. *Chem. Rev.* **1987**, *87*, 433−481. (e) Zimmerman, H. E.; Zhu, Z. *J. Am. Chem. Soc*. **1995**, *117*, 5245−5262.

(5) Hrovat, D.; Lieu, J. H.; Turro, N. J.; Wiess, J. D. G. *J. Am. Chem. Soc*. **1984**, *106*, 7033.

10.1021/ja9804767 CCC: $18.00
Published on Web 05/14/1999

reactions in microorganized media. In many instances, the chemoselectivity, regioselectivity, and/or stereoselectivity of chemical reactions can be enhanced.

Unfortunately, many of these systems suffer from various shortcomings that limit their ultimate practicality. Sol−gel derived (SGD) alumina exhibits many characteristics that make it an excellent material to explore as a microorganized medium to affect the selectivity of shape- and/or size-selective organic reactions. Thermal stability, chemical stability, mechanical stability, optical transparency, narrow pore size distribution, controllable pore size, and ease of thin film and monolith preparation are all characteristics of SGD-alumina that distinguish it from other microorganized media systems that, quite often, lack one or more of these desirable features.

In recent years, the synthesis and characterization procedures for SGD-alumina materials have been well-established. This work has examined the various aspects of hydrolysis, gel formation, and sintering conditions for the preparation of supported and unsupported alumina materials with controlled pore sizes and pore size distributions.[12] Although the results of this work have established many intricacies of SGD-alumina processing, these studies have focused on the application of SGD-alumina for separations and catalysis. However, the recent development of porous SGD-alumina as an effective separation medium and catalyst has produced a material with definitive pore sizes and shapes that more precisely confine organic molecules than alumina materials of the past. Earlier publications have presented the photochemistry and photophysics of adsorbed organic species on alumina and silica; however, the alumina and silica used in these studies are nonporous materials in which any effects are attributed to surface adsorption, rather than confinement within pores.[10] We report in this paper the first application of SGD-alumina as a microorganized medium in which surface adsorption and confinement within pores affects the selectivity of a chemical reaction.

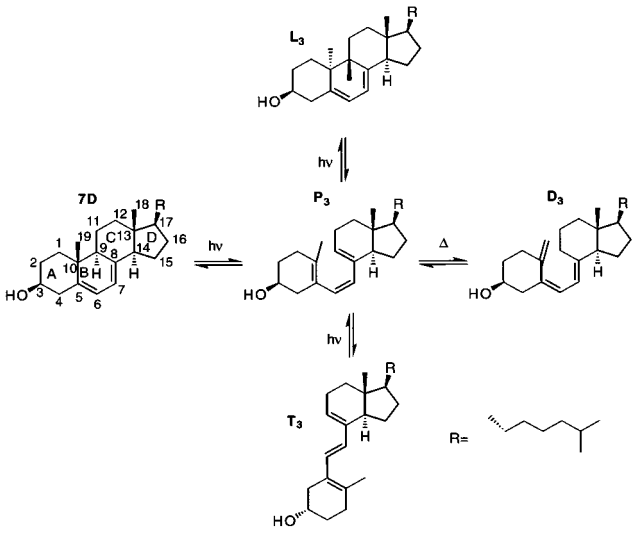

Figure 1. Photochemical and thermal isomerizations of D_3 isomers.

To examine the effectiveness of SGD-alumina as a microorganized medium, we studied the photochemical selectivity of 7-dehydrocholesterol (7D) encapsulated within the porous structure of SGD-alumina. Figure 1 shows the series of isomerizations that occur during the photochemical production of vitamin D (D_3) from 7D. The formation of D_3 begins with a photochemically allowed conrotatory electrocyclic ring opening of 7D yielding previtamin D_3 (P_3). P_3 is susceptible to conrotatory electrocyclic ring closure to 7D, conrotatory electrocyclic ring closure to lumisterol$_3$ (L_3), or cis−trans isomerization to tachysterol$_3$ (T_3). D_3 is produced from P_3 via a thermally allowed [1,7] sigmatropic hydrogen shift. Photolysis of 7D establishes a quasi-photostationary equilibrium between 7D, P_3, T_3, and L_3. Comprehensive studies have established the solution-phase photochemistry of 7D and the related isomers.[13] A key characteristic of the solution-phase photochemistry of 7D is the high selectivity toward T_3 at many photolysis wavelengths.[14] A tremendous amount of research effort has been directed toward understanding the photochemical selectivity of the vitamin D system and ultimately improving the selectivity toward previtamin D_3.

In attempts to control the selectivity of D_3 formation, several studies have examined the photochemistry of 7D in association with various microorganized media. These studies have included confinement of 7D within epidermal layers and synthetic phospholipid bilayers, adsorption to silica, and via micellar formation. Although various results have pointed toward an attenuation of T_3 formation, substantial discrepancies exist in the photochemical product distributions.[15−19] The ratio of P_3/

(6) (a) Lem, G.; Kaprinidis, N. A.; Schuster, D. I.; Ghatlia, N. D.; Turro, N. J.*J. Am. Chem. Soc.* **1993**, *115*, 7009. (b) Ramamurthy, V.; Eaton, D. F.; Casper, J. V. *Acc Chem. Res.* **1992**, *25*, 299. (c) Ramamurthy, V. In *Photochemistry in Organized and Constrained Media*; Ramamurthy, V., Ed.; VCH: New York, 1991; pp 429−493. (d) Ramamurthy, V.; Corbin, D. R.; Turro, N. J.; Zhang, Z.; Garcia-Garibay, M. A. *J. Org. Chem.* **1991**, *56*, 255−261. (e) Turro, N. J.; Cheng, C. C.; Abrams, L. Corbin, D. R. *J. Am Chem. Soc*. **1987**, *109*, 2449−2456.

(7) (a) Ogawa, M.; Kuroda, K. *Chem. Rev.* **1995**, *95*, 399−438. (b) Thomas, J. K. *Acc. Chem. Res.* **1988**, *21*, 275−280. (c) Usami, H.; Takagi, K.; Sawaki, Y. *Chem. Lett*. **1992**, 1405−1408.

(8) (a) Ramamurthy, V.; Eaton, D. F. *Acc. Chem. Res.* **1988**, *21*, 300. (b) Moorthy, J. N.; Venkatesan, K.; Wiess, R. G. *J. Org. Chem*. **1991**, *56*, 6957.

(9) (a) O'Brien, M. E.; Zimmerman, H. E. *J. Org. Chem.* **1994**, *59*, 1809−1816. (b) Horie, K.; Mita, I. *Adv. Polym. Aci*. **1989**, *88*, 77. (c) Guillet, J. Chapter 5. *Polymer Photophysics and Photochemistry*; Cambridge University Press: Cambridge, England, 1985.

(10) (a) Liu, Y. S.; de Mayo, P.; Ware, W. R. *J. Phys. Chem.* **1993**, *97*, 5995−6001. (b) Lednev, I. K.; Mathivanan, N.; Johnston, L. J. *J. Phys. Chem*. **1994**, *98*, 11444−11451. (c) Thomas, J. K. *Chem. Rev*. **1993**, *93*, 301−320. (d) Ford, W. E.; Kamat, P. V. *J. Phys. Chem.* **1989**, *93*, 6423−6428. (e) Johnston, L. J. Chapter 8. In *Photochemistry in Organized and Constrained Media*; Ramamurthy, V., Ed.; VCH: New York, 1991.

(11) (a) Al-Ekabi, H. In *Photochemistry in Organized and Constrained Media*; Ramamurthy, V., Ed.; VCH: New York, 1991; pp 495−534. (b) Fox, M. A. *Acc. Chem. Res.* **1983**, *16*, 314−321.

(12) (a) Yoldas, B. E. *Am. Ceram. Soc. Bull.* **1975**, *54*, 286−288. (b) Yoldas, B. E. *Am. Ceram. Soc. Bull.* **1975**, *54*, 289−290. (c) Yoldas, B. E. *J. Mater. Sci.* **1975**, *10*, 1856−1860. (d) Leenaars, A. F. M.; Burggraaf, A. J. *J. Colloid Interface Sci.* **1985**, *105*, 27−40. (e) Leenaars, A. F. M.; Keizer, K.; Burggraaf, A. J. *J. Mater. Sci.* **1984**, *19*, 1077−1088. (f) Hsieh, H. P.; Bhave, R. R.; Fleming, H. L. *J. Membr. Sci.* **1988**, *39*, 221−241. (g) Okubo, T.; Watanabe, M.; Kusakabe, K.; Morooka, S. *J. Mater. Sci.* **1990**, *25*, 4822−4827. (h) Uhlhorn, R. J. R.; Huis In't Veld, M. H. B. J.; Keizer, K.; Burggraaf, A. J. *J. Mater. Sci.* **1992**, *27*, 527−537. (i) Vendange, V.; Columban, Ph. *J. Mater. Res.* **1996**, *11*, 518−528. (j) Chane-Ching, J.-Y.; Klein, L. C. *J. Am. Ceram. Soc.* **1988**, *71*, 86−90. (k) Gieselmann, M. J. Ph.D. Thesis, University of Wisconsin−Madison, 1991.

(13) (a) Havinga, E.; Sanders, M.; Pot, J. *Fortchr. Chem. Org. Naturstoffen* **1969**, *29*, 131−157. (b) Verloop, A.; Koevoet, A. L.; Van Moorselaar, R.; Havinga, E. *Recueil* **1959**, 78, 1004−1016.

(14) (a) Havinga, E.; Jacobs, H.; Gielen, J. *Tetrahedron Lett.* **1981**, *40*, 4013−4016. (b) Dauben, W.; Phillips, R. *J. Am. Chem. Soc.* **1982**, *104*, 5780−5781.

(15) Holick, M. F.; MacLaughlin, J. A.; Doppelt, S. H. *Science* **1981**, *211*, 590−593.

(16) (a) Moriarity, R. M.; Schwartz, R. N.; Lee, C.; Curtis, V. *J. Am. Chem. Soc.* **1980**, *102*, 4257−4259. (b) Yamamoto, J. K.; Borch, R. F. *Biochemistry* **1985**, *24*, 3338−3344.

(17) Terenetskaya, I. P.; Perminova, O. G.; Yeremenko, A. M. *J. Mol. Struct.* **1990**, *219*, 359−364.

(18) Holick, M. F.; Richtand, N. M.; McNeill, S. C.; Holick, S. A.; Frommer, J. E.; Henley, J. W.; Potts, J. T., Jr. *Biochemistry* **1979**, *18*, 1003−1008.

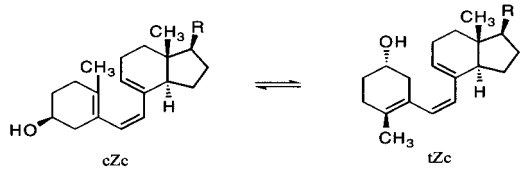

Figure 2. Prominent rotational conformations of P_3.

T_3 is highly dependent on the photolysis conditions; therefore, it is difficult if not completely inaccurate to compare results of one study to another without extreme attention given to experimental detail. Achievement of a photostationary-state, excitation wavelength, and attenuation of shorter wavelengths by the microorganized media are aspects of these results that are not definitive. In studies of human epidermal photolysis, careful attention was given to the irradiation wavelengths, and any effects on the product distribution were attributed to attenuation of shorter wavelengths by the stratum corneum rather than confinement effects.[20]

It is generally an accepted characteristic of the photochemistry of P_3 that the formation of T_3 arises predominately from the cZt rotamer, while the cZc rotamer leads to the formation of D_3 (see Figure 2). A recent computational study has addressed the photolysis selectivity for 7D adsorbed on silica on the basis of a substituent effect at position C3.[21] In this study the conformational selectivity between the cZc and cZt rotamer of P_3 is skewed toward the cZc rotamer by a bulky substituent at C3. These data suggests that adsorption of 7D to a silica surface via the 3-hydroxyl group would enhance the photochemical selectivity toward P_3. We will provide direct experimental evidence in this paper that demonstrates that neither H-bonding nor chemisorption via the 3-hydroxyl group to a SGD-alumina surface are sufficient to inhibit T_3 formation and affect the photochemical selectivity.

The results of the research presented in this paper have twofold importance: (1) This research demonstrates the first report of porous SGD-alumina functioning as an effective microorganized medium to alter the selectivity of an organic transformation that is confined within the porous structure of SGD-alumina. (2) The photochemical selectivity of the cis−trans isomerization of P_3 to T_3 can be greatly altered by the confining structure of SGD-alumina in conjunction with chemisorption. Adsorption alone via the 3-hydroxyl to the surface of a metal oxide such as SGD-alumina is not sufficient to inhibit the cis−trans isomerization of P_3 to T_3.

Experimental Section

Aluminum tri-*sec*-butoxide (ATSB) (97%) and 2-butanol (99%) were purchased from Aldrich Chemical Co. and used as received. 7-Dehydrocholesterol (Aldrich, 98%) was recrystallized from acetone. Purified water was obtained from a Barnstead NANOpore UV ultrapure water system. All solvents were of spectroscopic grade and were distilled from calcium hydride. Nitrogen adsorption/desorption analyses were performed with a Micromeritics ASAP 2010 instrument. Ultraviolet−visible spectra were obtained with a Hewlett-Packard 8452A spectrophotometer. Sol particles were sized by laser light scattering with a Brookhaven Instruments Corp. BI-2030AT digital correlator and BI-200SM goniometer equipped with a Lexal model 85 argon laser. Atomic force microscopy (AFM) images were obtained with a Digital Instruments Nanoscope III AFM/LFM instrument. Transmission electron microscopy (TEM) images were obtained with a JEOL 200CX microscope. Infrared (IR) spectra were recorded on a Nicolet Magna-IR 750 Series II infrared spectrometer. Loading concentrations of the SGD-alumina with 7D were determined with a Perkin-Elmer 2400 CHN elemental analyzer.

Porous SGD-Alumina: Boehmite (γ-AlOOH) Sol.[22] To 775 mL (43.1 mol) of purified water at 80 °C was added 187 mL of 2 M ATSB (0.374 mol) in 2-butanol. After refluxing and stirring for 2 h, 17 mL of 1.6 M nitric acid (0.0272 mol) was added. After another 2 h of refluxing and stirring, the condenser was removed and the 2-butanol was allowed to distill away. Once the distillation temperature reached 100 °C and the odor of 2-butanol was no longer present, the condenser was replaced and refluxing was continued overnight. The resulting sol was filtered sequentially with a Whatman GF/F glass fiber filter and a 0.45 μm Membra-Fil membrane filter (Fisher Scientific). Xerogels were formed in evaporating dishes constructed of optical quality acrylic plastic. The dishes were placed in desiccator boxes containing magnesium chloride hexahydrate as a drying agent. After 2 days of drying, the xerogels were sintered at 2 °C/min to 400, 700, or 950 °C. The resulting porous plates were 0.5 mm thick. Thin films of porous alumina were prepared by dip-coating with the alumina sol. By concentrating the freshly prepared sol by a factor of 3, 2 μm thick films of SGD-alumina were obtained on Pyrex or quartz glass supports. Film thickness was measured by profilometry and ultraviolet interference fringe patterns.

SGD-alumina plates (ca. 3 cm × 3 cm) were utilized for the photolysis experiments. The pore size of the SGD-alumina was varied by sintering the plates at 400, 700, and 950 °C to achieve slitlike pores of average widths of <20, <44, and 69 Å, respectively. Activation of the SGD-alumina involves removal of surface-adsorbed water at elevated temperatures in an atmosphere of air to generate a partially dehydroxylated surface in which Lewis acidic aluminum sites are exposed. For the incorporation of 7D, the plates were placed in a solution containing 7D dissolved in chloroform. In those experiments in which the plates were activated at 300 °C for 3 h, the plates were added directly from a furnace to the solution. After adsorption equilibrium was reached, the plates were removed from the solution, rinsed with fresh solvent, and evacuated for 4 h at 1 Torr. The plates were then placed in an immersion well photochemical apparatus (Ace Glass, Inc.). A Hanovia 400 W medium-pressure lamp was used for the photolysis experiments. A Vycor filter was used to isolate wavelengths greater than 240 nm.

The photolysis product distributions were determined with a Waters HPLC system equipped with a UV photodiode array detector. A Zorbax Sil column (4.6 mm i.d. × 25 cm) was used with a mobile phase of 0.4% 2-propanol in hexane with 0.05% water. UV spectral characteristics, retention time, and independent samples established peak identities. Since the desorption process required refluxing in ethanol, it was assumed that the formation of any D_3 was a result of thermal isomerization from P_3. The percentage of P_3 in the photolysis mixtures was taken as the summation of P_3 and D_3 amounts as determined by HPLC.

Results and Discussion

Characterization of the Particles and Pores of SGD-Alumina. The particle size distribution of the boehmite (γ-AlOOH) sols was determined by dynamic light scattering techniques. Figure 3 shows the size distribution of particles based on the relative number of particles obtained with the γ-AlOOH sol. From this figure it can be seen that the sol is composed of particles with diameters in the range 5−8 nm. The AFM images of the surface of SGD-alumina sintered at 400 °C are shown in Figure 4. The important features of these AFM images are the particle size and shape. From these images it can be seen that the particles are flat and oblong in shape, with dimensions of 6 × 10 nm across the face of the particle and a thickness of ca. 2 nm. The TEM micrograph of SGD-alumina is shown in Figure 5. This micrograph reaffirms the particle

(19) Terenetskaya, I. P.; Perminova, O. G.; Yeremenko, A. M. *J. Mol. Struct.* **1992**, *267*, 93−98.

(20) MacLaughlin, J. A.; Anderson, R. R.; Holick, M. F. *Science* **1982**, 216, 1001−1003.

(21) Dmitrenko, O.; Reischl, W. *Monatsch. Chem.* **1996**, *127*, 445−453.

(22) Gieselmann, M. J. Ph.D. Thesis, University of Wisconsin−Madison, 1991.

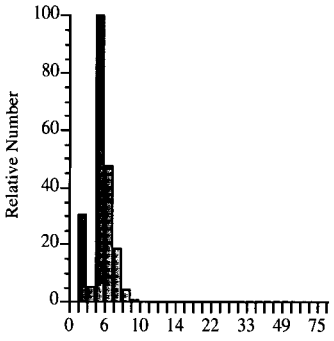

Figure 3. Relative number distribution of particle sizes in γ-A1OOH sol.

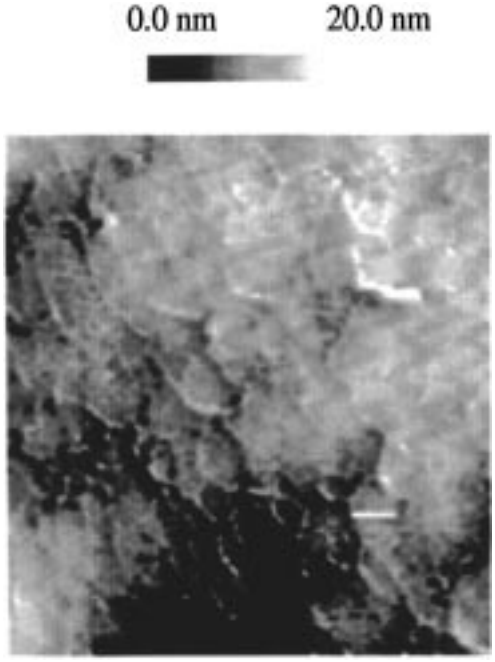

Figure 4. AFM image of SGD-alumina surface sintered at 400 °C. White bar = 6 nm.

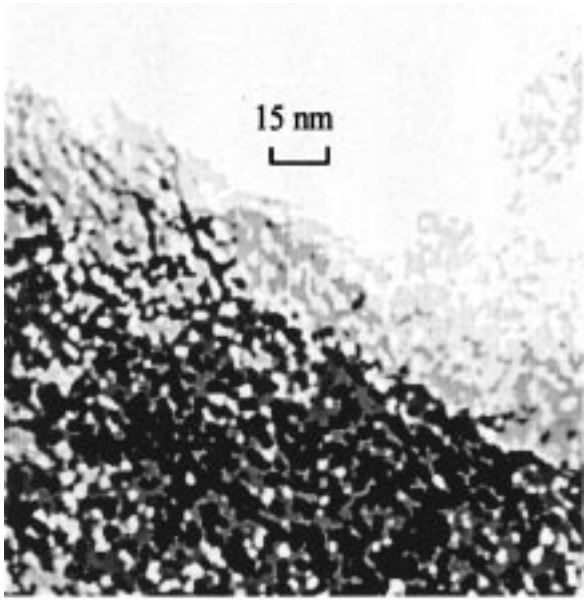

Figure 5. TEM micrograph of SGD-alumina sintered at 400 °C.

size as observed with the AFM image. From the TEM micrograph, the packing of ca. 6 nm particles can be observed.

Nitrogen Sorption Studies. The porous structure of SGD-alumina was characterized by utilizing data from nitrogen adsorption/desorption isotherms. Table 1 summarizes the characteristics of the porous structure obtained for SGD-alumina sintered at 400, 700, and 950 °C. The pore sizes were calculated from Brunauer, Emmett, and Teller (BET) desorption data using the Kelvin equation. These results reveal the relation between sintering temperature and pore size. Figure 6 presents the pore size distribution obtained from the Kelvin equation for SGD-alumina sintered at 400, 700, and 950 °C in which the corresponding average pore diameters are 36, 44, and 69 Å, respectively. The pore size distributions were obtained with the method of Barrett, Joyner, and Halenda (BJH) by utilizing the desorption data of the isotherm.[23] An important consideration with the pore widths determined for the SGD-alumina is the validity of the Kelvin equation at the pore dimensions present within the SGD-alumina of this study.[24] Studies have addressed this breakdown in the Kelvin equation and have quantified the error propagated through the calculations to derive a pore size distribution.[25] At pore diameters of less than 50 Å, the calculated values are inflated by more than 50%. Therefore, the reported pore size distributions in Figure 6 may be substantially elevated, especially the distribution for the 400 °C sintered sample that exhibits the smallest pore dimensions of the three samples. These pores are calculated to have a width of 36 Å, a value that may be inflated by more than 50%. On the basis of the approximate dimensions of the platelike particles as determined by AFM of $6 \times 10 \times 2$ nm, a slitlike pore width of 20 Å would be expected. The calculated average pore width for the 700 °C sintered SGD-alumina of 44 Å also falls in the region of uncertainty for the Kelvin equation. Although the uncertainty in this value is not as great as that for the 400 °C sintered SGD-alumina, the average pore width for the 700 °C sintered SGD-alumina would be expected to be much less than 44 Å.

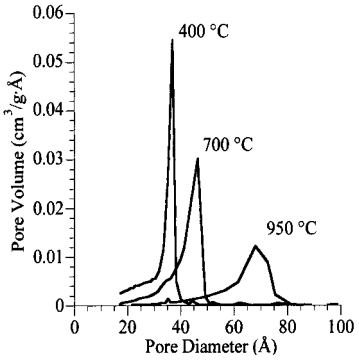

Figure 6. Pore size distribution for SGD-alumina sintered at 400, 700, and 950 °C based on the Kelvin equation and the method of BJH.

In the past few years, several computational methods have been developed that address the difficulties in obtaining pore size distributions of microporous materials. Horvath and Kawazoe[26] and Saito and Foley[27] have developed mean field methods that apply an average potential field across the adsorbate molecules in the pore for slit pores and cylindrical pores, respectively. The Horvath−Kawazoe method may provide a more accurate distribution for smaller slit-pore materials. Application of this model to the nitrogen sorption data reports a pore width of 10 Å. Therefore, for the SGD-alumina sintered

(23) Barrett, E. P.; Joyner, L. G.; Halenda, P. H. *J. Am. Chem. Soc.* **1951**, *73*, 373.
(24) Deleted in proof.
(25) Gregg, S. J.; Sing, K. S. W. *Adsorption, Surface Area and Porosity*, 2nd ed.; Academic: New York, 1982; p 152−154.
(26) Horvath, G.; Kawazoe, K. *J. Chem. Eng. Jpn.* **1983**, *16*, 470−475.
(27) Saito, A.; Foley, H. C. *AIChE J.* **1991**, *37*, 429−436.

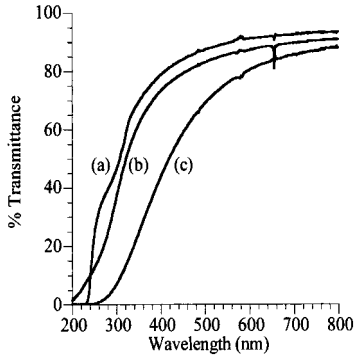

Figure 7. Optical transmission of SGD-alumina plates 0.5 mm thick sintered at (a) 400 °C, (b) 700 °C, and (c) 950 °C.

Table 1. Characteristics of the Porous Structure of SGD-Alumina Sintered at Various Temperatures

sintering temp (°C)	pore diameter (Å) Kelvin equation	BET surface area (m^2/g)	porosity (%)
400	36	251	47.7
700	44	175	47.7
950	69	87	41.5

Table 2. Final Adsorption Concentrations of 7D Adsorbed in Activated and Nonactivated SGD-Alumina Sintered at 400, 700, and 950 °C

	g of 7D/g of SGD-alumina	
sintering temp (°C)	no activation	activated at 300 °C
400	0.11	0.12
700	0.14	0.15
950	0.08	0.08

at 400 °C, the pore size distribution can be expected to be in the range 10−20 Å.

Optical Characteristics of SGD-Alumina. Figure 7 shows the UV−visible transmittance spectra for SGD-alumina sintered at 400, 700, and 950 °C. All of the materials exhibit excellent optical transparency through a broad range of wavelengths. As discussed above, one method of increasing the pore size in alumina is to increase the sintering temperature. From this figure it can be seen that, as the pore size increases with increased sintering temperatures, the low-wavelength cutoff exhibits a shift to longer wavelengths. This resulting shift is attributed to increased Rayleigh scattering from the larger pores and particles within the SGD-alumina structure.

Adsorption of 7-Dehydrocholesterol in SGD-Alumina. Table 2 presents the equilibrium adsorption concentration of 7D adsorbed on SGD-alumina sintered at 400, 700, and 950 °C. The specific surface areas for the SGD-alumina samples that were sintered at 400, 700, and 950 °C are 251, 175, and 87 m^2/g, respectively, as presented above. The final adsorption values for 7D indicate that adsorption is not directly related to the specific surface area of the SGD-alumina sample. We believe that this type of adsorption may arise if the pore dimensions in the 400 °C sample are too small to provide access for 7D. It is also possible that the adsorption of 7D in small pores occupies a greater amount of surface area than adsorption in larger pores. For smaller or narrower pores, the adsorption of 7D may be envisioned to occur in such a manner in which the cholesterol ring structure is essentially parallel to the surface of the platelike particle. For larger, or wider, pores, the surface adsorption of 7D may occur in a manner in which the cholesterol ring structure is perpendicular to the surface of the platelike particle. Calculation of the surface area occupied by each 7D molecule adsorbed within the SGD-alumina samples of different pore dimensions indicates that 7D adsorbs with a different geometric relation to the SGD-alumina surface. Relating the adsorption quantity of 7D to the surface area of the SGD-alumina produces the following surface area occupation values. For SGD-alumina sintered at 400, 700, and 950 °C, the surface area occupation values for 7D were 146, 80, and 70 $Å^2$ per 7D molecule, respectively. Molecular dimensions obtained from MM2[28] for 7D indicate that the cross-sectional areas for a plane perpendicular to the steroidal ring structure and a plane parallel to the ring structure are 40 and 120 $Å^2$, respectively. These values associated with the surface area occupation values indicate that the adsorption geometry of 7D is of a parallel nature for SGD-alumina sintered at 400 °C, while the adsorption geometry is of a perpendicular nature for SGD-alumina sintered at 700 and 950 °C (see Figures 13 and 14).

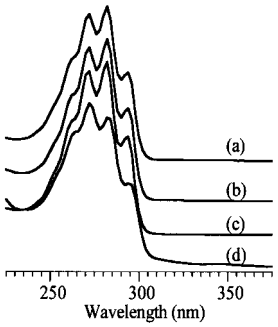

Figure 8. UV spectra of 7D in various media: (a) ethanol, (b) diethyl ether, (c) hexane, and (d) SGD-alumina.

The surface area requirement for adsorption indicates that the steroidal ring structure is parallel to the surface of the SGD-alumina that has been sintered at 400 °C. This type of adsorption geometry would also be expected for 7D adsorbed in a slitlike pore in which the pore width is narrow enough to prevent the perpendicular adsorption geometry as observed in the wider pores of the 700 and 950 °C sintered SGD-alumina. Earlier it was shown that the pore width for SGD-alumina sintered at 400 °C was in the range 10−20 Å. The longitudinal dimension of 7D is 17 Å as determined from MM2 calculations. These relative dimensions indicate that 7D would be required to adsorb in a more parallel manner for SGD-alumina sintered at 400 °C.

Electronic Interactions with Surface of SGD-Alumina. It has been reported in many instances that the photochemical reactivity and selectivity of organic molecules adsorbed on alumina or silica surfaces is affected by electronic interactions with the oxide surface.[10] Figure 8 shows the UV absorption spectra for 7D dissolved in various organic solvents and encapsulated within activated SGD-alumina. The absorbance maxima are at 262, 272, 282, and 294 nm for all of the systems. The difference in maximum intensities observed at lower wavelengths for the SGD-alumina system is attributed to light scattering by the porous structure of SGD-alumina. These UV data indicate that electronic interactions between the diene moiety of 7D and the surface of SGD-alumina are not prevalent.

Surface Adsorption Characteristics. Figure 9 shows the diffuse-reflectance IR spectra of 7D in the region of 2000−4000 cm^{-1}. Spectrum a results from 7D that has been encapsulated within nonactivated SGD-alumina. The OH stretching frequency occurs at 3471 cm^{-1}. Spectrum b results from a mixture of powdered SGD-alumina that has not been activated and powdered 7D. The OH stretching frequency occurs at 3495 cm^{-1}. As a comparison spectrum, spectrum c is a diffuse

(28) Allinger, N. L. *J. Comput. Chem.* **1993**, *14*, 755−768.

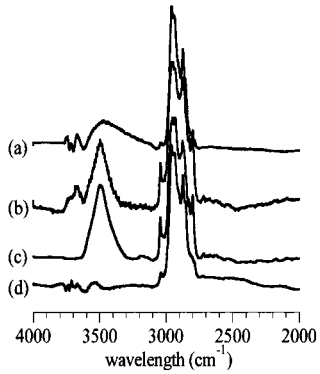

Figure 9. Diffuse-reflectance IR spectra of (a) 7D adsorbed on SGD-alumina, not activated, (b) 7D mixed with SGD-alumina, (c) 7D KBr pellet, and (d) 7D adsorbed on SGD-alumina, activated.

reflectance measurement of a KBr pellet of 7D. The OH stretching frequency for this spectrum remains at 3495 cm^{-1}. Spectrum d results from 7D that has been encapsulated from solution into activated SGD-alumina. The OH stretching band has essentially been eliminated.

The surface characteristics of alumina are significant in the binding that occurs between 7D and the SGD-alumina. Reported spectroscopic studies have indicated that activated alumina can cleave the heteroatom−H bond of alcohols and of primary and secondary amines with concomitant attachment of the alkoxide or amide groups to the alumina surface.[29] The diffuse-reflectance IR spectra shown in Figure 9 indicate that the 3-hydroxyl group of 7D is chemisorbed onto a coordinatively unsaturated Lewis acidic aluminum site on the surface of the activated SGD-alumina. However, on the SGD-alumina that has not been activated, the 3-hydroxyl group is hydrogen bonded to surface hydroxyl groups of the SGD-alumina. It has been shown that the surface hydroxyl groups of alumina serve as hydrogen bond donors rather than hydrogen bond acceptors.[30]

Desorption Characteristics. It was found that the desorption characteristics of 7D and its photoproducts were solvent- and temperature-dependent as expected for sorption processes. The greatest percent recovery was obtained in refluxing ethanol, in which the percent recovery after photolysis was essentially quantitative. Any unrecovered material is believed to be the result of the formation of the highly insoluble bischolestadienols. UV−visible spectral analysis of the plates after photolysis and extraction exhibits data characteristic of those reported for the bischolestadienols.[31]

Photolysis of 7D Encapsulated within SGD-Alumina. The effect on the product distribution obtained from the photolysis of encapsulated 7D in SGD-alumina was determined in relation to the product distribution obtained from the photolysis of 7D in hexane solution. The solution photochemistry of 7D in hexane with broad-band irradiation >240 nm is shown in Figure 10. The isomeric composition at the photostationary state as tabulated in Table 3 is 6% 7D, 52% P_3, 35% T_3, and 7% L_3.

Figures 11 and 12 show the percent composition of isomers as a function of time for the photolysis of 7D encapsulated in SGD-alumina that has been sintered at 400 °C. In this photolysis experiment, the loading level of 7D was 9.4% by mass and the SGD-alumina was not activated. These conditions represent the limiting conditions concerning the time required for attainment

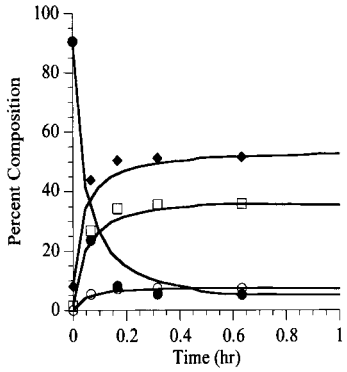

Figure 10. Percent composition of isomers on photolysis of 7D in hexane with Vycor filter: 7D (●), T_3 (□), P_3 (◆), and L_3 (○).

Table 3. Percent Compositions Resulting from the Photolysis of 7D Encapsulated in SGD-alumina of Different Pore Dimensions and Activation Conditions

SGD-alumina sintering temp (°C)	activation	% loading of 7D	% composition				
			7D	P_3	T_3	L_3	P_3/T_3
hexane			6	52	35	7	1.5
400	ambient	9.4	95	2.6	1.9	0.2	1.4
400	ambient	3.5	63	20	15	2	1.4
400	300 °C	8.9	96	3.4	0.3	0.2	11
400	300 °C	1.3	11	62	24	2.2	2.5
700	ambient	11	85	7.5	4.9	0.9	1.5
700	ambient	3.7	69	18	12	2.2	1.5
700	300 °C	1.4	57	26	15	4.2	1.7
700	300 °C	6.2	70	18	11	1.1	1.6
700	300 °C	12	95	3	1.3	0.3	2.3
950	300 °C	0.7	40	36	20	4.3	1.8
950	300 °C	6.9	84	10	5.0	0.8	2.0
950	ambient	6.9	76	15	7.8	1.2	1.9
950	ambient	1.9	34	38	23	4.9	1.7

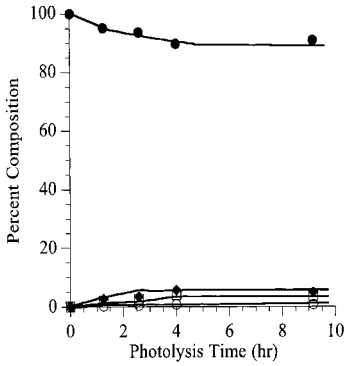

Figure 11. Percent composition of isomers on photolysis of 7D encapsulated in non-activated SGD-alumina sintered at 400 °C: 7D (●), T_3 (□), P_3 (◆), and L_3 (○).

of a photostationary state. From these figures it can be seen that the photostationary state is obtained after ca. 4 h of irradiation. For other systems in which the SGD-alumina was activated or the loading level was decreased, the achievement of a photostationary state occurred at shorter irradiation times. For subsequent SGD-alumina systems, the time required for achieving a photostationary state were independently determined. For systems at low loading levels, photolysis times of only several minutes were necessary for the achievement of a photostationary state. Table 3 summarizes the percent composition of the photostationary state obtained for the photolysis of 7D encapsulated in SGD-alumina of different pore dimensions, loading percentage, and activation condition.

We believe that the confinement effect on the product distribution from the photolysis of 7D is not solely a result of

(29) (a) DeCanio, E. C.; Nero, V. P.; Bruno, J. W. *J. Catal.* **1992**, *135*, 444−457. (b) Parera, J. M.; Figoli, N. S. *J. Catal.* **1969**, *14*, 303−304.

(30) Breton, G. W.; Daus, K. A.; Kropp, P. J. *J. Org. Chem.* **1992**, *57*, 6646−6649.

(31) Boomsma, F.; Jacobs, H. J. C.; Havinga, E.; Van Der Gen, A. *Recueil* **1973**, *92*, 1361−1367.

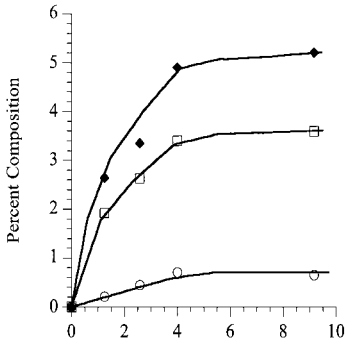

Figure 12. Percent composition of isomers on photolysis of 7D encapsulated in nonactivated SGD-alumina sintered at 400 °C: 7D (●), T_3 (□), P_3 (◆), and L_3 (○).

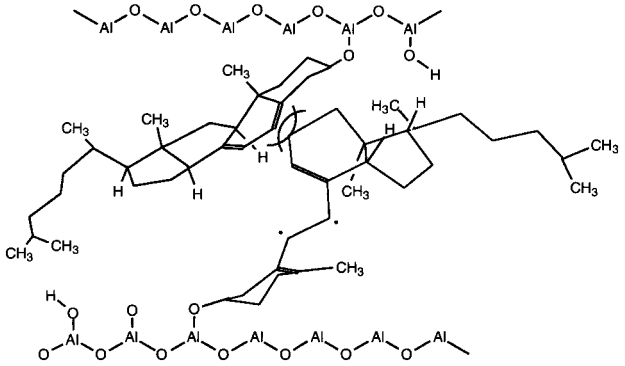

Figure 13. Steric interactions arising from the transition-state conformation required for cis−trans isomerization of P_3 to T_3 in SGD-alumina sintered at 400 °C and activated.

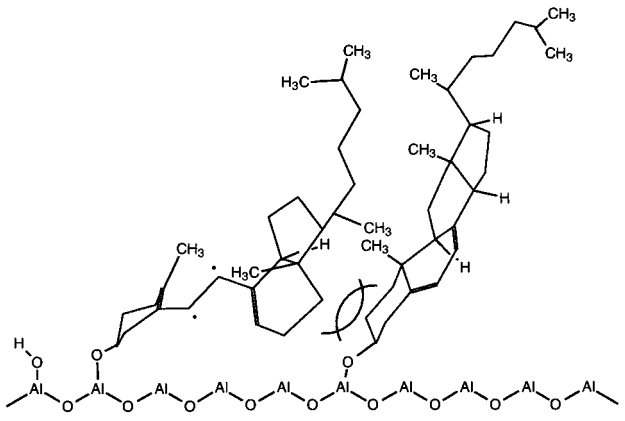

Figure 14. Steric interactions arising between co-adsorbed molecules in SGD-alumina sintered at 700 and 950 °C at the transition state required for cis−trans isomerization of P_3 to T_3.

adsorption or chemisorption of 7D to the SGD-alumina surface. For activated SGD-alumina sintered at 400 °C, we believe that the pore dimensions are small enough to inhibit the cis−trans isomerization of P_3 that is chemisorbed to the SGD-alumina surface (see Figure 13). Rotation about the C6−C7 bond can be accomplished by rotation of the A-ring or the C/D ring system or by a combination of rotation of these two systems. The anchoring of the A-ring by chemisorption at the 3-hydroxyl of 7D to the surface of the SGD-alumina requires rotation about the C6−C7 bond to be performed by the much larger C/D ring system of the cholesterol molecule. For 7D, which is hydrogen-bonded to the surface of the nonactivated SGD-alumina sintered at 400 °C, the surface adsorption is not strong enough to prevent rotation about the C6−C7 bond by the smaller A ring system of P_3. From these results it can be concluded that the pore dimensions of the 400 °C sample are not small enough to inhibit the rotation of the A ring system, but the pore dimensions are small enough to inhibit the rotation of the C/D ring system. For the 700 °C and 950 °C SGD-alumina, the pore dimensions of these materials are not capable of imposing sufficient confinement on P_3 to prevent the cis−trans isomerization to T_3.

At higher loading levels it is believed that 7D adsorbs to the surface of activated SGD-alumina sintered at 700 and 950 °C in a Langmuir−Blodgett manner. This arrangement at high loading levels provides sufficient confinement to inhibit the cis−trans isomerization to T_3. The source of confinement results from the proximity of surface-adsorbed molecules. The chemisorption through the 3-hydroxy group is important since it provides a source of restriction that does not exist in the nonactivated systems or the solid-state crystal system. At lower loading levels sufficient distance exists between the adsorbed molecules to allow the cis−trans isomerization to T_3.

For the 400 and 700 °C SGD-alumina that were not activated before adsorption, the P_3/T_3 ratio was essentially unchanged from that obtained with the solution photochemistry. The increase in the ratio with the nonactivated 950 °C SGD-alumina is attributed to excitation at longer wavelengths which greatly favors the formation of P_3.[14] Earlier it was shown that the larger pore 950 °C SGD-alumina exhibited a lower wavelength cutoff of ca. 300 nm.

In terms of conformational control, we believe that the formation of the tZc rotamer of P_3 is highly unfavorable for P_3 that is chemisorbed to the surface of SGD-alumina. Although the distribution of rotamers is highly shifted toward the cZc rotamer, we believe that the formation of T_3 occurs from the cZc conformation as demonstrated by those systems in which confinement is minimal. In a recent study of low-temperature photochemistry of P_3, it was noted that T_3 could arise from either conformer.[32] Our experimental evidence strongly supports this statement.

Solid-State Photolysis of 7D. It has been demonstrated by many researchers that the solid-state photochemistry of organic crystals can greatly affect product distributions when compared to the corresponding results of solution photochemistry.[4] These results are attributed to the crystal packing structure that forms a microorganized medium that restricts the conformational flexibility of the molecules during reaction. If the selectivity of the photochemistry of 7D is affected by confinement within a microorganized medium, then it is quite possible that the solid-state photochemistry of 7D would show deviations from the solution photochemical results. Since the photolysis of 7D is performed in the absence of solvent, the solid-state photoreactivity of 7D was also examined. Figure 15 shows the percent composition obtained for the photolysis of a film of 7D with light of wavelengths >240 nm. The films were prepared by dip-coating a glass tube in a concentrated solution of 7D dissolved in chloroform. The isomeric compositions are shown in Table 4. Since T_3 and P_3 are oils, on formation of these products any confinement integrity of the crystal structure would be expected to be greatly diminished. Since the product distribution on photolysis of 7D is directly dependent on the photochemistry of P_3, it may not be appropriate to consider this solid-state photochemistry. However, since the oil of P_3 is a condensed phase, it is quite possible that intrinsic confinement effects may affect the product distribution.

Although the results of the photolysis of 7D in the solid state indicate that different mechanistic concerns may affect the

(32) Müller, A. M.; Lochbrunner, S.; Schmid, W. E.; Fuss, W. *Angew. Chem., Int. Ed. Engl.* **1992**, *31*, 505−507.

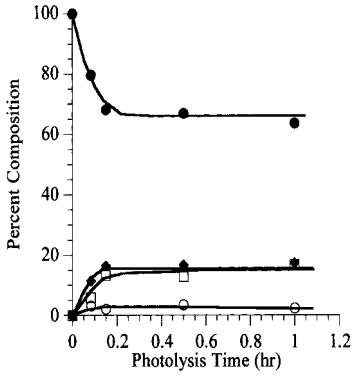

Figure 15. Photolysis of 7-dehydrocholesterol film with Vycor filter: 7D (●), T_3 (□), P_3 (◆), and L_3 (○).

Table 4. Percent Composition of Photolysis of 7D Film

	% composition				
photolysis medium	7D	P_3	T_3	L_3	P_3/T_3
hexane	6	52	35	7	1.5
7D thin film	64	17	17	2.4	1.0

product distribution, it can be concluded that the observed selectivity with the SGD-alumina system is not a direct consequence of solid-state or condensed-phase photochemistry. The SGD-alumina provides additional conformational flexibility control on 7D and the isomers derived from it.

Conclusion

The results presented in this paper demonstrate the first report of the ability of SGD-alumina to function as an effective microorganized media to alter the selectivity of an organic transformation. We have shown that the pore dimensions of activated SGD-alumina sintered at 400 °C, with pore dimensions of 10−20 Å, can inhibit the cis−trans isomerization of P_3 to T_3. Larger pore SGD-alumina sintered at 700 and 950 °C, with pore dimensions >20 Å, can also inhibit the cis−trans isomerization of P_3 to T_3 when the loading level of 7D is sufficiently high enough for coadsorbed molecules to impose an additional source of confinement. Although surface adsorption is expected to occur predominantly via the cZc rotamer of P_3, the presented results demonstrate that adsorption of 7D via the 3-hydroxyl in the absence of additional confinement is not sufficient to inhibit the cis−trans isomerization of P_3 to T_3.

Although SGD-alumina does possess many of the features required of a microorganized medium, some limitations do exist. In the case of photochemical reactions, "self-filtering" of light is a prominent limitation for highly concentrated systems. Also, scale-up of this methodology is at present a limitation. However, we expect that the flexibility in processing methods of sol−gel derived materials will allow the construction of flow through reactors that utilize thin films of the ceramic material. In the case of alumina, the surface can be catalytically active toward a variety of molecules and reactions. This activity can create other products, but in properly chosen systems, the activity can be utilized to promote desirable reactions. The size and shape of confining pores is obviously important to control size-selective reactions. We have found that the pore shape of SGD-alumina matches well to the space required to control the cis−trans isomerization of P_3 to T_3. Yet we do not expect any and all size-selective reactions to be affected by SGD-alumina. Current studies are exploring other classes of organic reactions with a variety of space requirements.

Acknowledgment. We thank the EPA through the Water Resources Center for funding of this project (Electrically Biased Photocatalytic Ceramic Membranes for Treatment of Impaired Waters). We thank Dr. Isabel Tejedor for her help with SGD-alumina production and IR interpretation.

JA9804767